

# Tolerance of topological surface states towards magnetic moments: Fe on $\text{Bi}_2\text{Te}_3$ and $\text{Bi}_2\text{Se}_3$

M. R. Scholz,<sup>1</sup> J. Sánchez-Barriga<sup>1</sup>, D. Marchenko,<sup>1</sup> A.

Varykhalov,<sup>1</sup> A. Volykhov,<sup>2</sup> L. V. Yashina,<sup>2</sup> and O. Rader<sup>1</sup>

<sup>1</sup>*Helmholtz-Zentrum Berlin für Materialien und Energie,*

*Elektronenspeicherring BESSY II, Albert-Einstein-Str. 15, D-12489 Berlin, Germany and*

<sup>2</sup>*Department of Chemistry, Moscow State University,*

*Leninskie Gory, 1/3, 119992 Moscow, Russia*

## Abstract

Topological insulators<sup>1-8</sup> are a novel form of matter which features metallic surface states with quasirelativistic dispersion similar to graphene<sup>9</sup>. Unlike graphene, the locking of spin and momentum and the protection by time-reversal symmetry<sup>1-8</sup> open up tremendous additional possibilities for external control of transport properties<sup>10-18</sup>. Here we show by angle-resolved photoelectron spectroscopy that the topological surface states of  $\text{Bi}_2\text{Te}_3$  and  $\text{Bi}_2\text{Se}_3$  are stable against the deposition of Fe without opening a band gap. This stability extends to low submonolayer coverages meaning that the band gap reported recently<sup>19</sup> for Fe on  $\text{Bi}_2\text{Se}_3$  is incorrect as well as to complete monolayers meaning that topological surface states can very well exist at interfaces with ferromagnets in future devices.

In contrast to most ordinary insulators, the bulk band gap of a topological insulator is caused by band inversion and strong spin-orbit coupling. Its surface is metallic due to nondegenerate and spin polarized surface states<sup>4-7</sup>. The spin is such that two surface-state electrons that propagate in opposite directions carry opposite spins. Owing to this spin chirality, electron backscattering by 180° is forbidden as it would require a spin flip. The surface state itself enjoys protection by time-reversal symmetry against distortions such as surface impurities<sup>4-7</sup>.

On the other hand, a magnetic field breaks time-reversal symmetry and by lifting the degeneracy  $E(\uparrow) = E(\downarrow)$  causes a gap in the topological surface state at zero momentum in inversion-symmetric systems. This has been proven in transport measurements by applying 28 mT to a HgTe-based two-dimensional quantum spin Hall system<sup>8</sup>. For a three-dimensional topological insulator, much more efficient than an external field is the use of the exchange field from a deposited ferromagnet. For such configuration, numerous electronic effects have been predicted<sup>10-18</sup> such as the quantized topological magnetoelectric effect leading to half-integer charges at magnetic domain boundaries<sup>10,11</sup> a magnetoresistance increasing for parallel (sic!) domain magnetizations<sup>12</sup>, and an inverse spin-galvanic effect enabling the dissipationless magnetization reversal by an applied electrical current<sup>13</sup>.

While these effects are awaiting experimental verification, much progress has recently been made in the identification of appropriate topological three-dimensional insulator materials, starting with Bi10%Sb<sup>20</sup>. The second generation of three-dimensional topological insulators, Bi<sub>2</sub>Se<sub>3</sub> and Bi<sub>2</sub>Te<sub>3</sub><sup>2,27,30</sup> forms particularly simple systems with the topological surface state appearing as a single Dirac cone at the  $\bar{\Gamma}$ -point of the surface Brillouin zone, i. e., for  $k_{\parallel} = 0$ , and a substantial spin polarization<sup>30</sup> which has been shown to approach 100%<sup>21,22</sup>. The band gaps are large enough to allow for room-temperature applications but as-grown samples show a tendency for defects (e. g., excess Te on Bi sites) which lead to a *n*-type bulk doping so large that the samples are rendered metallic in their bulk.

Several studies have investigated the effect of magnetic moments on the topological surface state. When Bi<sub>2</sub>Se<sub>3</sub> is doped with Fe in the bulk, a gap opens in the surface-state dispersion at Fe concentrations (relative to Bi) from 5% to 25%<sup>23</sup>. This includes concentrations for which the system remains paramagnetic down to low temperatures ( $T = 2$  K), such as 12% Fe, where the surface-state band gap amounts to 45 meV<sup>23</sup>. When Bi<sub>2</sub>Se<sub>3</sub> is p-doped in the bulk by Mn, it is possible to move the bulk band gap to the Fermi level<sup>23</sup>. Bulk Mn

doping of  $\text{Bi}_2\text{Te}_3$  and  $\text{Sb}_2\text{Te}_3$  has led to ferromagnetic order below temperatures of 10 K and 17 K, respectively. Unfortunately, photoemission of the Dirac point region remained inconclusive, possibly due to the strong p-doping<sup>25</sup>.

Most recently, Fe deposited directly on the surface of  $\text{Bi}_2\text{Se}_3$  has been studied by means of angle-resolved photoemission<sup>19</sup>. It was revealed that the Fe dopes the surface substantially beyond its self-doping and opens at submonolayer coverages a surface-state band gap of 100 meV. The authors speculate that the topological surface state mediates<sup>26</sup> an out-of-plane anisotropy of the Fe magnetic moments without long-range ferromagnetic order<sup>19</sup>.

In the present Letter, we investigate the behavior of  $\text{Bi}_2\text{Te}_3$  and  $\text{Bi}_2\text{Se}_3$  upon Fe deposition. We characterize the system Fe/ $\text{Bi}_2\text{Te}_3$  systematically by angle-resolved photoemission of the valence band and by photoemission of the Bi 5d, Te 4d, and Fe 3p core levels. In agreement with previous work<sup>19</sup> we observe energy shifts of the surface band structure consistent with electron doping. We find that we can shift the Dirac point for both systems by not more than 150 meV which is much less than what was reported previously. Most strikingly we show direct evidence that the Dirac crossing remains intact even under heavy Fe deposition and that in no stage of Fe deposition a band gap opens.

For  $\text{Bi}_2\text{Te}_3$  we monitor the evolution of the surface state band structure with 55 eV photons at room temperature after each deposition step of Fe. Panel a of Figure 1 shows the  $E(\mathbf{k})$  dispersion relations of the topological surface state along the  $\overline{\text{M}}-\overline{\Gamma}-\overline{\text{M}}$  direction of the surface Brillouin zone (see inset) with a red dashed line showing the shift of the Dirac point with increasing Fe deposition. In the pristine sample (top left, 0 ML) we see the V-shaped dispersion of the topological surface state like in previous work<sup>28</sup>. The Dirac crossing point is clearly visible at the present photon energy where the intensities of the two branches appear to add up. The Dirac point lies in a dip of the bulk valence band projection at 200 meV binding energy which has its origin in the band inversion<sup>27</sup>. Furthermore, the surface bands hybridize for symmetry reasons<sup>21</sup> with the bulk bands at  $\overline{\Gamma}$  which follow an upward dispersion but appear weak like in previous work<sup>28,30</sup>.

Figure 1 shows for 0.1 ML Fe an increasing background and the appearance of a well defined Fermi edge due to Fe 3d states. Surface bands have shifted rigidly towards higher binding energies by 96 meV. At the center of the surface Brillouin zone the bottom of a new, parabolic shaped band appears at 20 meV binding energy. By increasing the amount of Fe the band structure shifts further to higher binding energies with the deposited mass

following an exponential-like behaviour (Fig. 2a). Around 0.3 ML Fe we achieve saturation of the surface doping. The shift of the Dirac point reaches 150 meV and can also be followed for normal-electron-emission ( $\bar{\Gamma}$ ) spectra in the inset of Fig. 2a. (The appearance of a shoulder at the high-binding-energy side of the Dirac point will be discussed further below in connection with our low-temperature measurements.)

Figure 1b shows the effect of Fe deposition on the topological surface state of  $\text{Bi}_2\text{Se}_3$ . 18 eV photons are used which enhances the contrast between bulk and surface states as compared to 55 eV. Again, the band structure undergoes a shift consistent with n-type surface doping. The region of the bulk conduction band, situated in between the two branches of the topological surface state, alters in a peculiar way. At 0.1 ML Fe the Dirac point has shifted by 100 meV, considerably less than the  $> 300$  meV shift assigned previously to this coverage<sup>19</sup>. More importantly, the shift saturates at 140 meV for 0.3 ML.

As can be seen in Figure 2b the Bi 5d and Te 4d core levels exhibit a similar shift as the Dirac point. However, while the Te 4d states shift much stronger and the shift does not seem to saturate even at 1 ML Fe coverage, the Bi 5d states shift even less than the Dirac point but saturate at a similar coverage. The black curve in the upper inset shows the spin-orbit split  $5d_{3/2}$  and  $5d_{5/2}$  core-level peaks at 27.6 eV and 24.55 eV binding energies, respectively. (For better comparability, a Shirley background has been subtracted and the spectra have been normalized to the same area.)

In addition to the shift to higher binding energies, shoulders become with increasing Fe amount visible at the lower binding energy side of each Bi 5d peak (see also inset). The stoichiometry of  $\text{Bi}_2\text{Te}_3$  demands the Bi atoms to be in the 3+ oxidation state (2- for Te) so that the two shoulders are assigned to Bi with lower oxidation state than 3+. Since the topmost layer of the (00·1) cleavage plane is made up of Te atoms<sup>31</sup>, the Fe is expected to react with Te. The newly formed bonds between Fe and Te lead to a weakening of the interlayer bonding between Te and Bi atoms of the topmost two atomic layers of the substrate. This is followed by a strengthening of the intra-layer bonding between Bi atoms of the second layer which causes the chemical shift. To confirm that the observed changes are really due to Fe, we show the growing Fe 3p core level in Fig. 2c for different coverages. The Bi 5d states in  $\text{Bi}_2\text{Se}_3$  show the same strong changes as can be seen in Fig. 2d. This leads to the same microscopic picture as compared to  $\text{Bi}_2\text{Te}_3$ . It should be emphasized that Fig. 2d reports a

fairly strong chemical interaction of Fe with the substrate against which the surface state of the substrate remains topologically protected. This insensitivity is worthwhile mentioning in addition to those towards disorder, Coulomb and magnetic perturbations.

The analysis of the Se 3d peak is not straightforward since the Fe 3p resides approximately at the same binding energy and in addition to growth of this peak underneath we expect changes due to the chemical reaction similar as in the Te 4d states. There are indeed similarities like an energy shift and an asymmetry at the higher binding energy side. The difference is a change in the relative intensities of the Se 3d<sub>3/2</sub> and the Se 3d<sub>5/2</sub> peak. We normalized to equal Se 3d<sub>5/2</sub> intensity to emphasize that the Se 3d<sub>3/2</sub> peak contains the additional Fe 3p spectral weight.

To investigate the effect of the Fe adatoms on the surface electronic structure in more detail and to enable the suggested out-of-plane alignment of Fe moments induced at low temperatures by the topological surface state<sup>19</sup>, we have cooled the Fe-covered sample down to  $T = 50$  K for Bi<sub>2</sub>Te<sub>3</sub> and 8 K for Bi<sub>2</sub>Se<sub>3</sub>. Upon cooling, the Dirac point has been found to shift to larger binding energies between 50 and 100 meV. This effect is visible in the core-level spectra and reverses after warming up. This may be due to temporary residual gas adsorption. It is clearly seen in Fig. 3a that the Dirac point remains intact. The second derivative data of 0.4 ML Fe shows in addition that the Dirac point as the origin of the linearly dispersing topological surface state stays connected to the bulk band. In the second derivative, also an M-shaped dispersive band is resolved which is separated from the Dirac point at  $\bar{\Gamma}$  by 100 to 200 meV.

In Bi<sub>2</sub>Se<sub>3</sub> we again observe a similar picture (Fig. 3b). We are able to resolve a pair of M-shaped bands in the second derivative which are well separated from the Dirac point. No gap has opened at the Dirac point which is in clear contradiction to the previous observation<sup>19</sup>.

Finally we want to turn to the extra states close to the Fermi level. In Fig 3d we show the Fermi surface of Bi<sub>2</sub>Te<sub>3</sub> measured with 21 eV photons at low temperature. At this energy extra states which cannot be seen well at 55 eV due to unfavourable photoemission cross section are seen to appear in the cut along the  $\bar{K}$ - $\bar{\Gamma}$ - $\bar{K}$  direction. We find two nested parabolas with the bottom of the lower band at 60 meV binding energy. We also observe a pair of nested parabolas in Bi<sub>2</sub>Se<sub>3</sub>. In the previous work, a stronger doping-induced

energy shift was observed and a pronounced  $\mathbf{k}_{\parallel}$  splitting of Rashba type was resolved<sup>19</sup>. Our doping induced shifts saturate instead at 140 meV and no Rashba-type spin-orbit splitting is seen in the well-resolved bands. In a most recent work, extra states at the Fermi energy have been obtained instead of volutary deposition by just exposing the surface of  $\text{Bi}_2\text{Se}_3$  to residual gas<sup>32</sup>. Their formation has been explained as a two-dimensional electron gas due to a quantum well at the surface of  $\text{Bi}_2\text{Se}_3$  due to band bending<sup>32</sup>. For the present experiment this means that it is especially important not to cross contaminate the surface by other species during the Fe deposition experiments.

In conclusion, we find that the topological surface state of  $\text{Bi}_2\text{Te}_3$  is tolerant against magnetic adsorbates not only at low coverages but at least up to the limits of detectability by angle resolved photoemission which lie around 1 ML for  $\text{Bi}_2\text{Te}_3$  in the present experiment. This means that  $\text{Bi}_2\text{Te}_3$  can be interfaced with a ferromagnet without losing the topological surface state and its unique dispersion. For  $\text{Bi}_2\text{Se}_3$  we achieve the same conclusion thus contradicting the gap opening reported before. We show that Fe reacts chemically when deposited on the surface which gives additional emphasis to the unique robustness of topological surface states. The presently found robustness is the precondition for the exploration and the successful functionalization of interfaces between topological insulators and ferromagnets. This will involve growing a perpendicularly magnetized ferromagnetic film on top of a topological insulator and monitoring the effect of the exchange coupling on the topological surface state underneath.

## Methods

Single crystals of  $\text{Bi}_2\text{Te}_3$  and  $\text{Bi}_2\text{Se}_3$  were grown by the Bridgman method. Small portions of the crystal have been cut and prepared with copper adhesive tape for *in situ* cleavage resulting in (00·1) surfaces in hexagonal coordinates. Angle-resolved photoemission measurements have been carried out in ultra high vacuum of  $1 \cdot 10^{-10}$  mbar with a Scienta R8000 electron analyzer at the UE112-PGM2a beam-line of BESSY II with p polarized undulator radiation. Fe was deposited *in situ* from an e-beam oven with the sample kept at room temperature. The evaporation rate has been repeatedly calibrated with a quartz

microbalance and was typically 0.05 ML/min.

---

- <sup>1</sup> C. L. Kane, E. J. Mele, Quantum spin Hall effect in graphene, *Phys. Rev. Lett.* 95, 146802 (2005);  $Z_2$  topological order and the quantum spin Hall effect, *Phys. Rev. Lett.* 95, 226801 (2005).
- <sup>2</sup> Liang Fu, C. L. Kane, Topological Insulators with inversion symmetry, *Phys. Rev. B* 76, 45302 (2007).
- <sup>3</sup> B. A. Bernevig, S. C. Zhang, Quantum spin Hall effect, *Phys. Rev. Lett.* 96 106802 (2006).
- <sup>4</sup> Liang Fu, C. L. Kane, E. J. Mele, Topological insulators in three dimensions, *Phys. Rev. Lett.* 98, 106803 (2007).
- <sup>5</sup> J. E. Moore, L. Balents, Topological invariants of time-reversal-invariant band structures, *Phys. Rev. B* 75, 121306 (2007).
- <sup>6</sup> R. Roy, Topological phases and the quantum spin Hall effect in three dimensions, *Phys. Rev. B* 79, 195322 (2009).
- <sup>7</sup> S. Murakami, Phase transition between the quantum spin Hall and insulator phases in 3D: emergence of a topological gapless phase, *New J. Phys.* 9, 356 (2007).
- <sup>8</sup> M. König, S. Wiedmann, C. Brüne, A. Roth, H. Buhmann, L. W. Molenkamp, X.-L. Qi, S.-C. Zhang, Quantum spin hall insulator state in HgTe quantum wells, *Science* 318, 766 (2007).
- <sup>9</sup> E. Rotenberg, Topological insulators: The dirt on topology, *Nature Phys.* 7, 8 (2011).
- <sup>10</sup> X. L. Qi, T. L. Hughes, S. C. Zhang, Fractional charge and quantized current in the quantum spin Hall state, *Nature Phys.* 4, 273-276 (2008)
- <sup>11</sup> X. L. Qi, T. L. Hughes, S. C. Zhang, Topological field theory of time-reversal invariant insulators, *Phys. Rev. B* 78, 195424 (2008)
- <sup>12</sup> T. Yokoyama, Y. Tanaka, N. Nagaosa, Anomalous magnetoresistance of a two-dimensional ferromagnet/ferromagnet junction on the surface of a topological insulator, *Phys. Rev. B* 81, 121401 (2010).
- <sup>13</sup> I. Garate, M. Franz, Inverse Spin-Galvanic Effect in the Interface between a Topological Insulator and a Ferromagnet *Phys. Rev. Lett.* 104, 146802 (2010).
- <sup>14</sup> S. Mondal, D. Sen, K. Sengupta, R. Shankar, Tuning the Conductance of Dirac Fermions on the Surface of a Topological Insulator, *Phys. Rev. Lett.* 104, 046403 (2010).

- <sup>15</sup> Zhenhua Wu, F. M. Peeters, Kai Chang, Electron tunneling through double magnetic barriers on the surface of a topological insulator Phys. Rev. B 82, 115211 (2010).
- <sup>16</sup> Ya Zhang, Feng Zhai, Tunneling magnetoresistance on the surface of a topological insulator with periodic magnetic modulations, Appl. Phys. Lett. 96, 172109 (2010).
- <sup>17</sup> A. A. Burkov, D. G. Hawthorn, Spin and Charge Transport on the Surface of a Topological Insulator, Phys. Rev. Lett. 105, 066802 (2010).
- <sup>18</sup> B. D. Kong, Y. G. Semenov, C. M. Krowne, K. W. Kim, Unusual magnetoresistance in a topological insulator with a single ferromagnetic barrier, Appl. Phys. Lett. 98, 243112 (2011).
- <sup>19</sup> L. A. Wray, S. Y. Xu, Y. Xia, D. Hsieh, A. V. Fedorov, Y. San Hor, R. J. Cava, A. Bansil, H. Lin, M. Z. Hasan, A topological insulator surface under strong Coulomb, magnetic and disorder perturbations, Nature Physics 7, 32-37 (2010)
- <sup>20</sup> D. Hsieh, D. Qian, L. Wray, Y. Xia, Y. S. Hor, R. J. Cava, M. Z. Hasan, A topological Dirac insulator in a quantum spin Hall phase, Nature 452, 970-975 (2008)
- <sup>21</sup> M. R. Scholz, D. Marchenko, A. Varykhalov, A. Volykhov, L. V. Yashina, O. Rader, High spin polarization and circular dichroism of topological surface states on Bi<sub>2</sub>Te<sub>3</sub>, Phys. Rev. Lett. (under review)
- <sup>22</sup> Z.-H. Pan, E. Vescovo, A. V. Fedorov, D. Gardner, Y. S. Lee, S. Chu, G. D. Gu, T. Valla, Electronic Structure of the Topological Insulator Bi<sub>2</sub>Se<sub>3</sub> Using Angle-Resolved Photoemission Spectroscopy: Evidence for a Nearly Full Surface Spin Polarization, Phys. Rev. Lett. 106, 257004 (2011)
- <sup>23</sup> Y. L. Chen, J. H. Chu, J. G. Analytis, Z. K. Liu, K. Igarashi, H. H. Kuo, X. L. Qi, S. K. Mo, R. G. Moore, D. H. Lu, M. Hashimoto, T. Sasagawa, S. C. Zhang, I. R. Fisher, Z. Hussain, Z. X. Shen, Massive Dirac fermion on the surface of a magnetically doped topological insulator, Science 329, 5992 (2010).
- <sup>24</sup> J. Choi, S. Choi, J. Choi, Y. Park, H.-M. Park, H.-W. Lee, B.-C. Woo, S. Cho, Magnetic properties of Mn-doped Bi<sub>2</sub>Te<sub>3</sub> and Sb<sub>2</sub>Te<sub>3</sub>, Physica Status Solidi (B) 241, 1541 (2004).
- <sup>25</sup> Y. S. Hor, P. Roushan, H. Beidenkopf, J. Seo, D. Qu, J. G. Checkelsky, L. A. Wray, D. Hsieh, Y. Xia, S.-Y. Xu, D. Qian, M. Z. Hasan, N. P. Ong, A. Yazdani, R. J. Cava, Development of ferromagnetism in the doped topological insulator Bi<sub>2-x</sub>Mn<sub>x</sub>Te<sub>3</sub>, Phys. Rev. B 81, 195203 (2010)
- <sup>26</sup> Q. Liu, C.-X. Liu, C. Xu, X.-L. Qi, S.-C. Zhang, Magnetic Impurities on the Surface of a Topological Insulator Phys. Rev. Lett. 102, 156603 (2009)

- <sup>27</sup> H. Zhang, C.-X. Liu, X.-L. Qi, Xi Dai, Z. Fang, S.-C. Zhang, Topological insulators in  $\text{Bi}_2\text{Se}_3$ ,  $\text{Bi}_2\text{Te}_3$  and  $\text{Sb}_2\text{Te}_3$  with a single Dirac cone on the surface, *Nature Physics* 5 (6), 438-442 (2009).
- <sup>28</sup> Y. L. Chen, J. G. Analytis, J.-H. Chu, Z. K. Liu, S.-K. Mo, X. L. Qi, H. J. Zhang, D. H. Lu, X. Dai, Z. Fang, S. C. Zhang, I. R. Fisher, Z. Hussain, Z.-X. Shen, Experimental Realization of a Three-Dimensional Topological Insulator,  $\text{Bi}_2\text{Te}_3$  *Science* 325, 5937 (2009).
- <sup>29</sup> Y. Xia, D. Qian, D. Hsieh, L. Wray, A. Pal, H. Lin, A. Bansil, D. Grauer, Y. S. Hor, R. J. Cava, M. Z. Hasan, Observation of a large-gap topological-insulator class with a single Dirac cone on the surface, *Nature Physics* 5 (6), 398-402 (2009).
- <sup>30</sup> D. Hsieh, Y. Xia, D. Qian, L. Wray, J. H. Dil, F. Meier, J. Osterwalder, L. Patthey, J. G. Checkelsky, N. P. Ong, A. V. Fedorov, H. Lin, A. Bansil, D. Grauer, Y. S. Hor, R. J. Cava, M. Z. Hasan, A tunable topological insulator in the spin helical Dirac transport regime, *Nature* 460, 7259 (2009).
- <sup>31</sup> R. W. G. Wyckoff, *Crystal Structures*, Wiley, New York, 1964, vol. 2.
- <sup>32</sup> M. Bianchi, D. Guan, S. Bao, J. Mi, B. B. Iversen, P. D. C. King, P. Hofmann, Coexistence of the topological state and a two-dimensional electron gas on the surface of  $\text{Bi}_2\text{Se}_3$ , *Nature Communications* 1, 128 (2010).

**FIG. 1. Behaviour of topological surface states upon deposition of Fe.** Angle-resolved photoemission data at room temperature for (a)  $\text{Bi}_2\text{Te}_3$  and (b)  $\text{Bi}_2\text{Se}_3$ . The red dashed line follows the surface doping effect on the Dirac point. The Dirac point is clearly observed at the employed photon energies of (a) 55 eV and (b) 18 eV.

**FIG. 2. Substantial doping and chemical interaction from core-level spectroscopy.** (a) The surface doping of  $\text{Bi}_2\text{Te}_3$  from normal-emission valence-band spectra (inset) is roughly in agreement with the core-level shifts of (b) Bi 5d and Te 4d, except for Fe 3p of the dopant (c). (d) The shoulders of Bi 5d reflect a substantial chemical interaction. (e) The Fe 3p signal is hidden under Se 3d in  $\text{Bi}_2\text{Se}_3$ .

**FIG. 3. The topological surface state at low temperature.** Fe deposition at room temperature does not open a gap in the topological surface state on (a)  $\text{Bi}_2\text{Te}_3$  at 50 K and (c)  $\text{Bi}_2\text{Se}_3$  at 8 K. The Fe-induced states at the Fermi energy appear as a pair in (c)  $\text{Bi}_2\text{Se}_3$  and in (b)  $\text{Bi}_2\text{Te}_3$  when measured at low photon energies (21 eV) where also their strong warping is revealed. Also the valence band becomes split as revealed by two M-shaped dispersions. This does not affect the Dirac crossing point of the topological surface state.

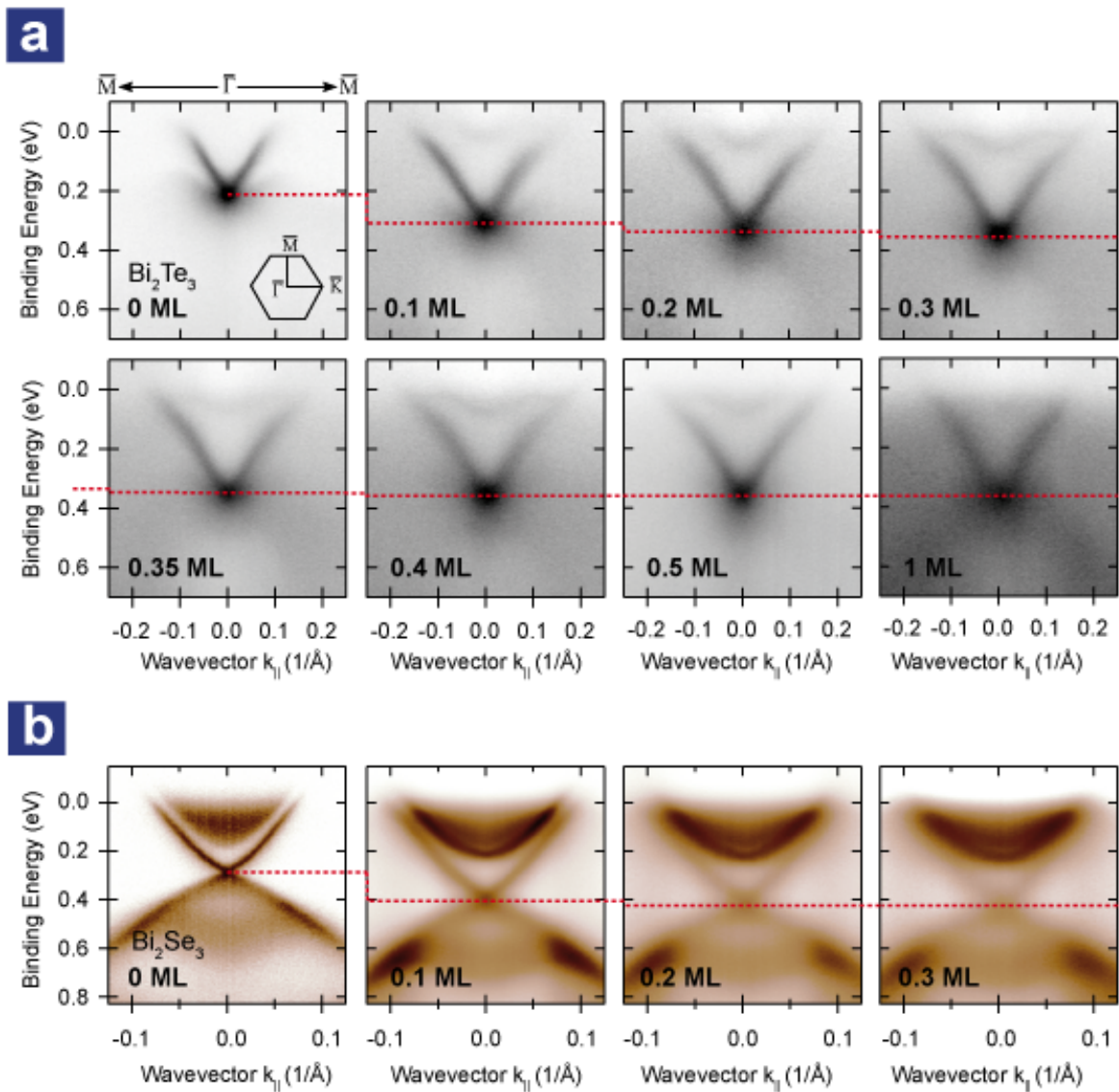


**Figure 1**

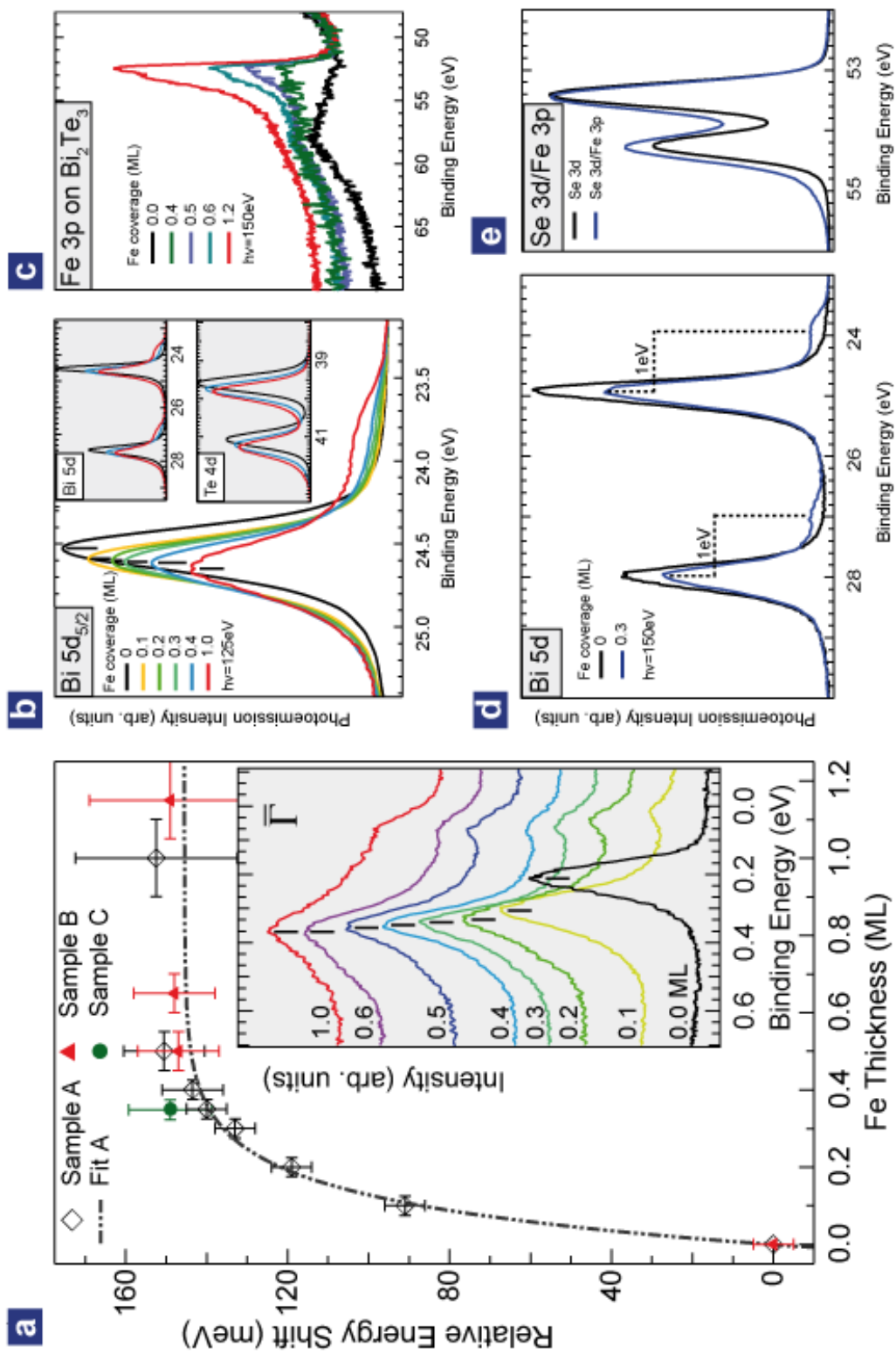


**Figure 2**

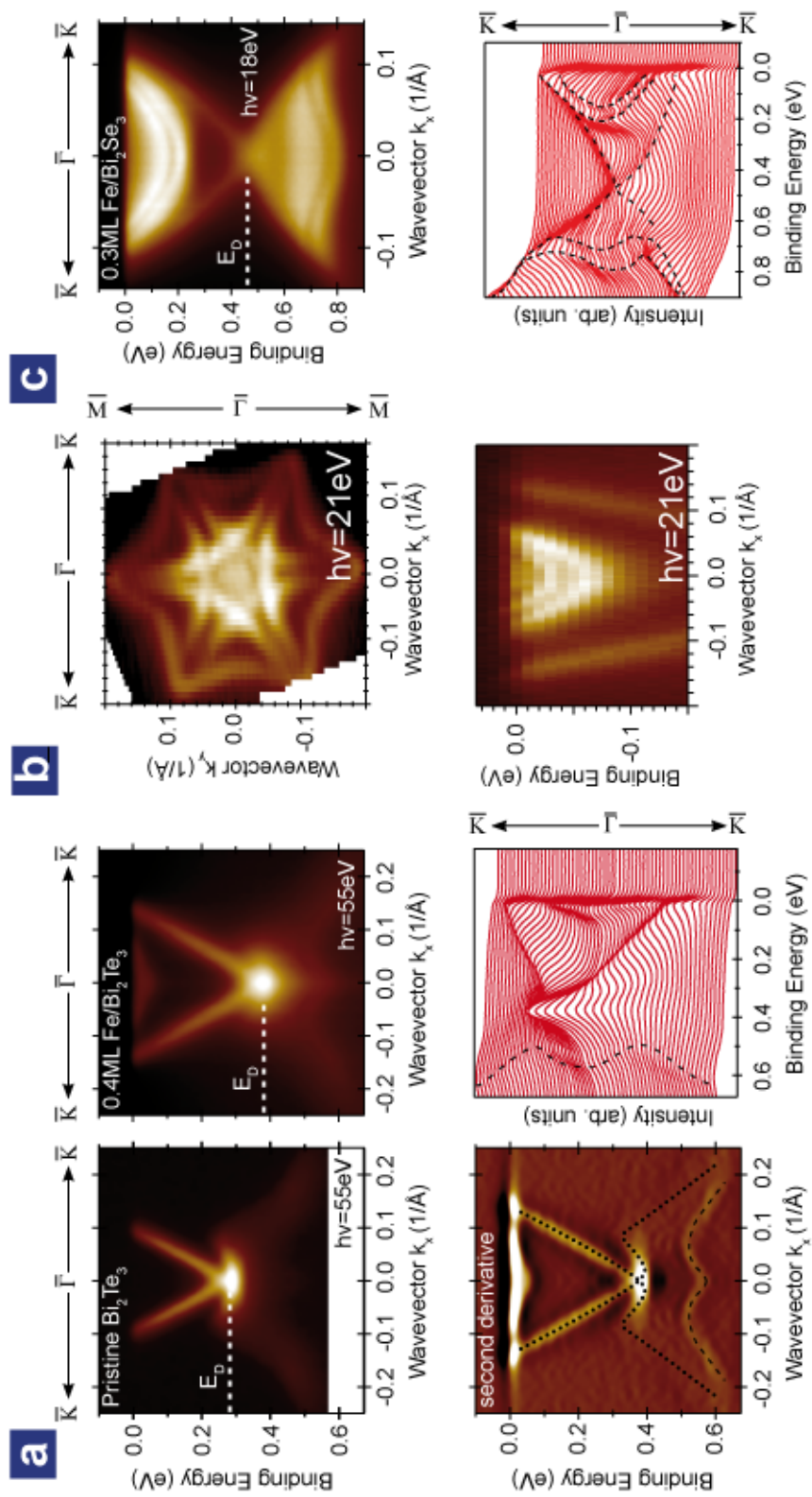


**Figure 3**